

Discovery of an activity cycle in the solar-analog HD 45184[★]

Exploring Balmer and metallic lines as activity proxy candidates

M. Flores^{1,5}, J. F. González^{1,3,5}, M. Jaque Arancibia^{1,5}, A. Buccino^{2,4,5}, and C. Saffe^{1,3,5}

¹ Instituto de Ciencias Astronómicas, de la Tierra y del Espacio (ICATE), España Sur 1512, CC 49, 5400 San Juan, Argentina. e-mail: mflores, fgonzalez, mjaque, csaffe@icate-conicet.gob.ar

² Instituto de Astronomía y Física del Espacio (IAFE), Buenos Aires, Argentina. e-mail: abuccino@iafe.uba.ar

³ Facultad de Ciencias Exactas, Físicas y Naturales, Universidad Nacional de San Juan, San Juan, Argentina.

⁴ Departamento de Física, Facultad de Ciencias Exactas y Naturales, Universidad de Buenos Aires, Buenos Aires, Argentina.

⁵ Consejo Nacional de Investigaciones Científicas y Técnicas (CONICET), Argentina.

Received September 15, 1996; accepted March 16, 1997

ABSTRACT

Context. Most stellar activity cycles similar to that found in the Sun have been detected by using the chromospheric Ca II H&K lines as stellar activity proxies. However, it is unclear if such activity cycles could be identified using other optical lines.

Aims. To detect activity cycles in solar-analog stars and determine if these can be identified through other optical lines, such as Fe II and Balmer lines. We study the solar-analog star HD 45184 using HARPS spectra, whose temporal coverage and the high quality of the spectra allow us to detect both long and short-term activity variations.

Methods. We analyse the activity signatures of HD 45184 by using 291 HARPS spectra obtained between 2003 and 2014. In order to search for line-core fluxes variations, we focus on Ca II H&K and Balmer H α , H β lines, which are usually used as optical chromospheric activity indicators. We calculate the HARPS-S index from Ca II H&K lines and convert it to the Mount-Wilson scale. In addition, we also consider as activity indicators the equivalent widths of Balmer lines. Moreover, we analyse the possible variability of Fe II and other metallic lines in the optical spectra. The spectral variations are analysed for periodicity using the Lomb-Scargle periodogram.

Results. We report for the first time a long-term 5.14-yr activity cycle in the solar-analog star HD 45184 derived from Mount Wilson S index. This makes HD 45184 one of most similar stars to the Sun with known activity cycle. Such variation is also evident in the first lines of the Balmer series, which not always show a correlation with activity in solar-type stars. Notably, unlike the solar case, we also found that the equivalent widths of the high photospheric Fe II lines (4924 Å, 5018 Å and 5169 Å) are modulated (± 2 mÅ) by the chromospheric cycle of the star. These metallic lines show variations above 4σ in the RMS spectrum, while some Ba II and Ti II lines present variations at 3σ level which could be considered as marginal variations. From short-term modulation of the S index we calculate a rotational period of 19.98 days, which agrees with its mean chromospheric activity level. Then, we clearly show that the activity cycles of HD 45184 could be detected in both Fe II and Balmer lines.

Key words. stars: activity – stars: chromospheres – stars: solar-type – stars: individual: HD 45184

1. Introduction

The pioneer research on stellar activity by Wilson (1978) and subsequent works (e.g. Vaughan et al. 1978; Duncan et al. 1991; Gray & Baliunas 1995) have allowed to better understand the activity phenomenon beyond the Sun. A major contribution on this subject was made by Baliunas et al. (1998), who analysed the flux variability of Ca II H&K lines and found three different types of behaviour. They found cycles with periods between 2.5 and 25 yr often associated to stars with moderate activity. Very active stars displayed fluctuations of activity rather than cycles, while inactive stars seem to be in a state similar to the solar Maunder-minimum, the time period between the years 1645 and 1715, when the Sun deviated from its usual 11-year activity cycle.

Since pioneering surveys to date, several stellar cycles have been reported (e.g. Hall et al. 2007; Metcalfe et al. 2010; DeWarf et al. 2010; Metcalfe et al. 2013; Buccino et al. 2014;

Egeland et al. 2015). These works identified activity cycles in stars of spectral types F to M (even stars with exoplanets), including stars with multiple cycles. The Ca II H&K lines are commonly used as optical activity proxies (e.g. Baliunas & Jastrow 1990; Baliunas et al. 1998; Hall et al. 2007), as well as other lines such as those of the Balmer series (Robertson et al. 2013a; Reiners et al. 2012) or the Mg II infrared triplet (see e.g. Busà et al. 2007; Pietarila & Livingston 2011). However, it is unclear if the activity cycles could be identified using other optical lines. Such activity cycles have important implications in different fields. For instance, studying a range of stars with physical characteristics similar to the Sun across a range of age and other parameters is very useful to understand how typical the Sun is (e.g. Hall et al. 2007, 2009), and in particular the frequency of Earth-influencing behaviors (e.g. Maunder minimum). Importantly, the discovery of activity cycles also helps to disentangle stellar and planetary signals in radial-velocity surveys (e.g. Robertson et al. 2013b; Carolo et al. 2014).

We started a program aiming to detect activity cycles in solar-analog stars using the extensive database of HARPS spec-

[★] Based on data products from observations made with ESO Telescopes at the La Silla Paranal Observatory under programs 072.C-0488 and 183.C-0972.

tra. Our initial sample comprises close solar-analog stars taken from Nissen (2015), who carefully selected stars with physical parameters very similar¹ to the Sun (± 100 K in T_{eff} , ± 0.15 dex in $\log g$, and ± 0.10 dex in $[\text{Fe}/\text{H}]$) and also requiring spectra with very high signal-to-noise S/N (≥ 600). The similarity between these stars and the Sun, together with the possibility to have spectra with high S/N and an homogeneous parameter determination, encouraged us to initially select these objects. However, we do not discard the future possible inclusion of more stars in order to extend our sample.

An inspection of the preliminary data showed a notable variation in the chromospheric activity of the G1.5V (Gray et al. 2006) star HD 45184 (= HR 2318, $V = 6.39$, $B-V = 0.62$). It is located at a distance of ~ 22 pc (van Leeuwen 2007) and hosts a debris disk of $1-2 M_{\oplus}$ (Lawler et al. 2009). The reported fundamental parameters are $T_{\text{eff}} = 5871 \pm 6$ K, $\log g = 4.445 \pm 0.012$ dex, $[\text{Fe}/\text{H}] = 0.047 \pm 0.006$ dex and $v_{\text{turb}} = 1.06 \pm 0.017$ km s⁻¹ (Nissen 2015). He also derived a mass of $1.06 \pm 0.01 M_{\odot}$ (only internal error) and age of 2.7 ± 0.5 Gyr, showing that HD 45184 is ~ 1.8 Gyr younger than the Sun. Then, with the aim to detect possible activity cycles, we collected all the available HARPS spectra for this object. Multiple observations are required to properly identify both long and short-term activity variations. For the case of HD 45184, we gathered a total of 291 spectra covering more than 10 years of observations, being then a very good target to search for a possible activity cycle. HD 45184 has been also identified as a candidate to host a planetary mass companion of $0.04 M_{\text{Jup}}$ detected by radial velocity (Mayor et al. 2011), and is included in the Extrasolar Planets Encyclopaedia². These facts place HD 45184 as a very interesting object and encouraged us to perform the study presented here.

This work is organized as follows. In Section §2 we describe the observations and data reduction, while in Section §3 we describe our results and finally in Section §4 we outline our discussion.

2. Observations and data reduction

The spectra were obtained from the European Southern Observatory (ESO) archive³, under the ESO programs 072.C-0488(E) (PI: M. Mayor and S. Udry) and 183.C-0972(A) (PI: S. Udry). The observations were taken with the HARPS spectrograph attached to the La Silla 3.6m telescope between 2003 to 2014 and have been automatically processed by the HARPS pipeline⁴. The spectra have a resolving power $R \sim 115\,000$ and cover the spectral range 3782–6913 Å. After discarding a few low signal-to-noise observations we obtained a total of 291 spectra with a mean signal-to-noise $S/N \sim 175$ at 6490 Å.

Since this work was intended to search for low-level flux variations, the spectra were carefully normalized and cleaned. Cosmic rays were identified and removed considering a threshold of 5 times the noise level. Continuum differences between the spectra were corrected by filtering low-frequency modulations.

Telluric features were removed dividing each observed spectrum S_{obs} by an empirical telluric spectrum T appropriately

¹ Strictly speaking, this is a sample of "solar-analog stars" rather than "solar-twins" as was called by Nissen, given that (for instance) the age interval covered was 0.7 - 8.8 Gyr.

² <http://exoplanet.eu/>

³ <https://www.eso.org/sci/facilities/lasilla/instruments/harps/tools/archive.html>

⁴ <http://www.eso.org/sci/facilities/lasilla/instruments/harps/doc.html>

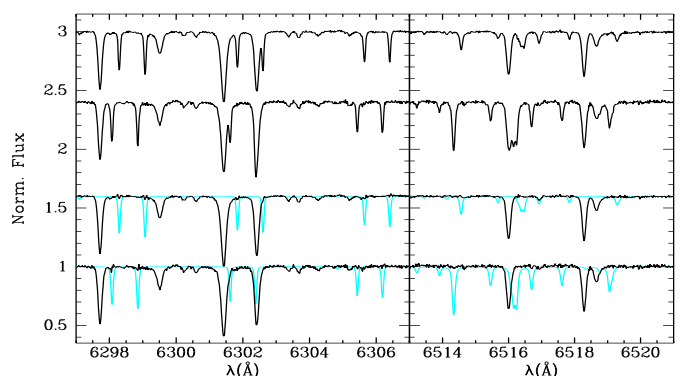


Fig. 1. Removal of telluric lines. For two observations of different runs the original spectra are shown on the top. Below the clean spectra (black) are overlotted with the telluric model spectra used in each case (light blue).

scaled:

$$S_{\text{corr}} = S_{\text{obs}} \cdot T^{-\alpha},$$

where α represents the relative optical thickness of the terrestrial atmosphere. This coefficient α was chosen to reproduce the telluric line intensities, most of which are due to water vapour in our spectral region. We repeat this procedure using a template of the O₂ γ -band around 6300 Å. In this way we were able to correct satisfactorily observations taken with different atmospheric water vapour content. Figure 1 shows an example of the removal of telluric lines in two small spectral windows. Telluric lines in the left panel correspond to atmospheric O₂, while in the right panel are due to H₂O.

3. Results

3.1. Chromospheric Ca II H&K lines

HARPS-S index was obtained following the classical method used to calculate the Mount Wilson S index (Vaughan et al. 1978). We integrated the flux in two windows centred at the cores of the Ca II H&K lines (3933.664 Å and 3968.470 Å), weighting with triangular profiles of 1.09 Å FWHM. The ratio of these fluxes to the mean continuum flux was computed by using two 20 Å wide passbands, centred at 3891 Å and 4011 Å. Finally, we derived the Mount Wilson S index by using the calibration procedure explained in Lovis et al. (2011).

In Figure 2 we plot the time series of the original 291 HARPS measurements. The total uncertainty σ_{tot} of individual S determinations were derived by adding quadratically both the observational error σ_{obs} (obtained as in Henry et al. 1996), and the systematic error associated to the calibration between HARPS and Mt Wilson activity indexes ($\sigma_{\text{sys}} \sim 0.0043$, according to Lovis et al. 2011). For clarity, error bars corresponding to σ_{tot} are not shown in Fig. 2, being almost identical for all points. In addition to the individual measurements, we include in the Fig. 2 the average values of observations associated to the same observing season. Error bars of the average values correspond to the standard deviation of the mean. For the case of bins with one measurement, we adopted the typical RMS dispersion of other bins. Both time series show a clear evidence of a chromospheric activity cycle. Applying the Lomb-Scargle periodogram (Horne & Baliunas 1986) to the seasonal means, we derived a period $P = 1878 \pm 9$ days (~ 5.14 yr). We used seasonal means in this analysis in order to reduce the rotational scatter, as

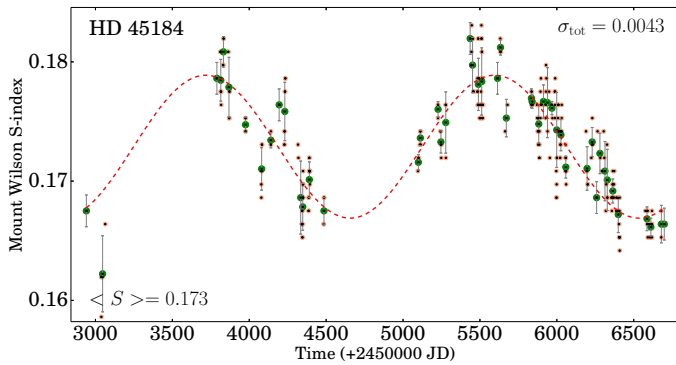


Fig. 2. Time series of Mount Wilson index measurements of HD 45184 from full HARPS data set (small orange circles) and seasonal means (big green circles). The dotted red line indicates the cycle calculated in this work. The probable error of individual measurements is about 0.0043.

is usual (e.g. Baliunas et al. 1995; Gomes da Silva et al. 2011). The False Alarm Probability (FAP) corresponding to the main peak is 3.1×10^{-07} .

Along with the observational data, Fig. 2 shows the harmonic curve of period 1878 days (red dotted line), obtained as the least-square fit to the seasonal means with a confidence level of 99% (see Buccino & Mauas 2009, for details). The semi-amplitude of the fitted curve is $\Delta S = 0.0062 \pm 0.0002$ and the epoch of maximum activity corresponds to JD 2,455,600.

The mean Mount Wilson index of HD 45184 obtained in this work is $\langle S \rangle = 0.173$ is undistinguishable from the values derived by Henry et al. (1996, $\langle S \rangle = 0.173$) and Gray et al. (2006, $\langle S \rangle = 0.172$). The mean activity level of HD 45184 is therefore similar to that of the Sun ($\langle S \rangle_{\odot} = 0.171$, Hall et al. 2009).

3.2. Balmer and metallic lines as activity indicators

Several studies have suggested that the correlation between the chromospheric emission from the Ca II H&K and H α lines present in Sun (Livingston et al. 2007) could be found in other stars (e.g. Meunier & Delfosse 2009; Martínez-Arnáiz et al. 2010, 2011; Stelzer et al. 2013; Gomes da Silva et al. 2014). Even though this correlation has been reported as not always valid (Cincunegui et al. 2007), the activity in the Sun and other stars measured by Ca II H&K emission could correlate with other chromospheric and even high photospheric lines (e.g. Hall & Lockwood 1998; Livingston et al. 2007).

To search for such correlations, we looked for possible variations in H I and metallic lines in the spectra using different techniques. On the one hand we averaged the 291 spectra and built an RMS spectrum by calculating at each wavelength the RMS of residuals. Before these calculations, a mild filter in low and high-frequencies was applied to the residual spectra in order to remove continuum differences and reduce shot noise. Since shot noise is an important contribution to the observed RMS, strong lines present in general a RMS value lower than the surroundings. For this reason, we divided the RMS spectrum by the theoretical noise-level spectrum calculated from photon statistics.

As a second strategy, we applied the technique of Sokolov (2000). In this case, all the flux measurements at a given wavelength are used to produce a light curve that is fitted by least-squares with the first terms of a Fourier series. In our study, we fixed the period and derived at each wavelength the amplitude of the flux variation assuming a sinusoidal function.

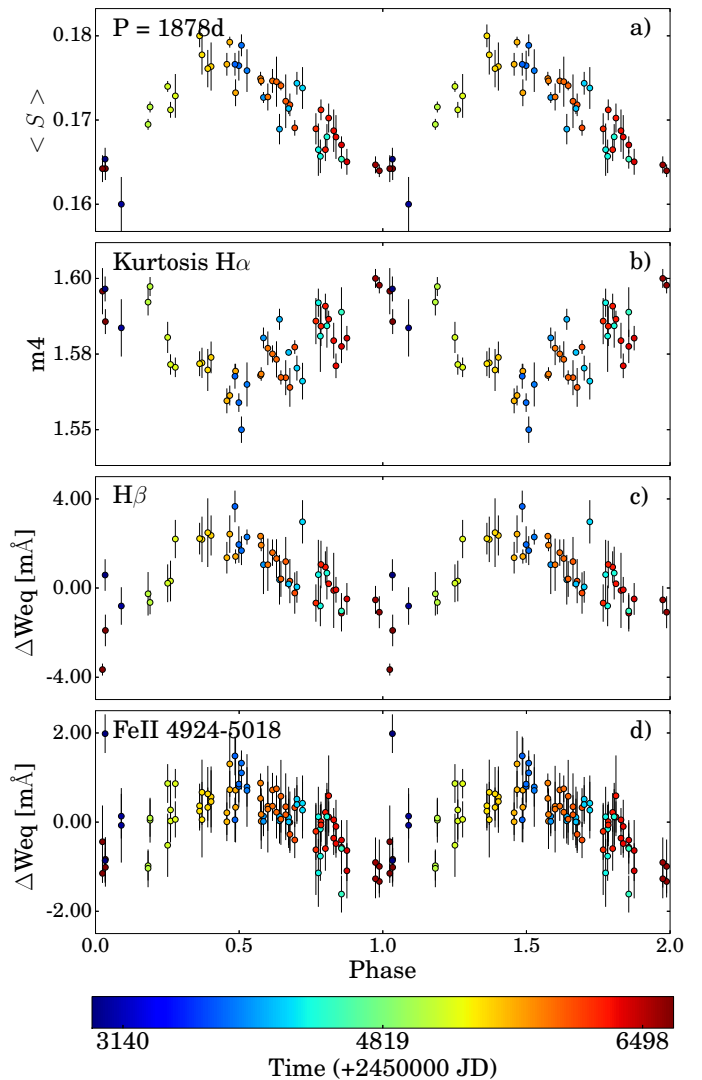


Fig. 4. a) Chromospheric activity measurements from Ca II H&K lines. b) kurtosis of the H α line. c) and d) panels correspond to the equivalent width of Balmer H β , Fe II 4924 Å and Fe II 5018 Å lines. Phases have been calculated with a period of 1878 days.

From this analysis we detected, besides Ca II lines, significant variations near the core of H I lines and in some strong iron lines, particularly Fe II lines at 4924 Å, 5018 Å and 5169 Å. Figure 3 shows the RMS spectrum and the light-variation amplitude spectrum for small spectral windows around selected lines. The amplitude and RMS spectra have been normalized to the mean noise level in the region. All mentioned lines (Ca II H&K, H β , H α , Fe II 4924 Å, 5018 Å and 5169 Å) present variations above 4σ , with flux variations of about 0.6% of the continuum level. Additionally, a few other lines of ionized metals exhibit variations at a 3σ level, which we consider here as marginal detections. These lines are the Ba II line at 6141.8 Å and Ti II lines at 4395.0 Å, 4443.8 Å, 4468.5 Å, 4501.3 Å, and 4572.0 Å. In these cases, flux variations are about 0.4–0.5% of the continuum.

To study the temporal behaviour we derived equivalent width variations by integrating the residual spectra around the central wavelength of the variable lines. Figure 4 shows the Mount Wilson S index along with the equivalent width of H I and Fe II lines as a function of the activity cycle phase. There is a clear correlation between the intensity of the lines and the chromospheric

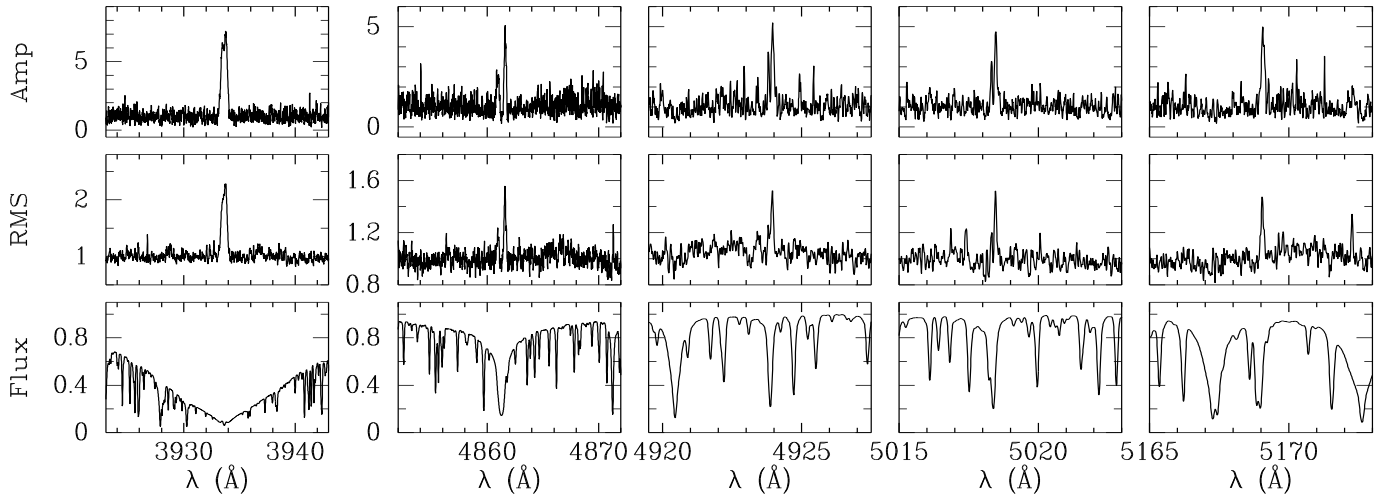


Fig. 3. Spectral variability. Light-variation amplitude spectrum (upper panels) and RMS spectrum (middle panels) are shown for small spectral windows around 5 variable spectral lines: Ca II 3933, Fe II 4924, Fe II 5018, and Fe II 5169. Lower panels show the average spectrum in each region.

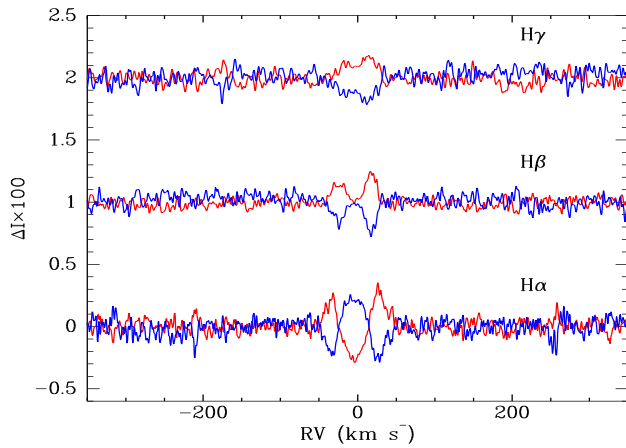


Fig. 5. Difference of Balmer line profiles for high (blue) and low (red) activity phases.

activity, for the lines H β , Fe II 4924 Å, and Fe II 5018 Å. In the case of H α , even though the spectral variability of the line core (± 1 Å around the line center) is out of doubt, there are no noticeable net changes in the equivalent width. This is evident in Fig. 5, where we compare the average of 85 residual spectra close to the low activity phase (blue) and the average of 57 spectra around the activity maximum (red). To quantify the spectral variations in H α we calculated the kurtosis of the line core, in a spectral window of 4 Å. The resulting values show the same behaviour as other activity indicators as shown in the second panel of Fig. 4. Then, Balmer and Fe II lines variations reproduce the 5.14-yr activity cycle detected with the Mount Wilson index, although with lower amplitude-to-error ratio. This is confirmed by the corresponding periodograms (Fig. 6) in which all the highest peaks lie between 1877 and 1879 days (the Mount Wilson indexes, the kurtosis of H α , and the flux of H β and Fe II lines).

3.3. Rotation period

As is often the case in other magnetic stars, the point spread in the chromospheric activity curve is significantly larger than the estimated measurement errors, what can be attributed to ro-

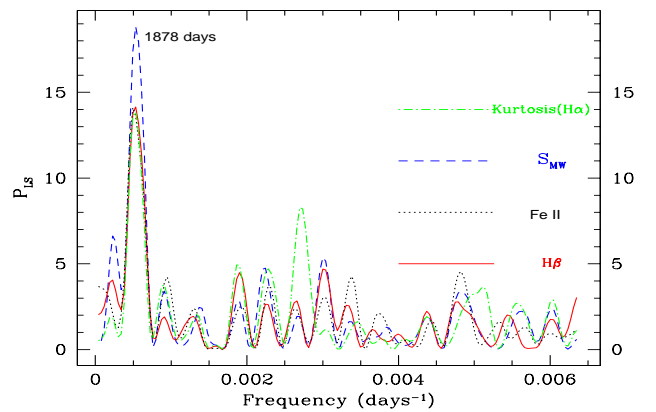


Fig. 6. Lomb-Scargle periodogram from the different line variations plotted in Fig. 4.

tational modulations caused by passage of individual active regions (Gray & Baliunas 1995; Brown et al. 2008; Metcalfe et al. 2010). To detect such variations and to determine the rotation period, we have followed a strategy similar to Metcalfe et al. (2010). We subtract from the individual measurements of the S index the fitted harmonic curve (red dotted line in Fig. 2) and analyse the periodicity of the residuals by using both the Lomb-Scargle periodogram and the Phase Dispersion Minimization technique (Stellingwerf 1978).

As a result, we found a period of 19.98 ± 0.02 days with a very low FAP = 1.04×10^{-11} for the S index. This analysis was based in Ca II lines. The signal-to-noise ratio of the variations found in other lines is too low to be used for the rotational analysis. Figure 7 shows the periodogram and the S-index residuals as a function of phase. Our result is in agreement with the period estimated by Wright et al. (2004) (21 days) using the empirical relation between rotation and chromospheric activity calibrated by Noyes et al. (1984).

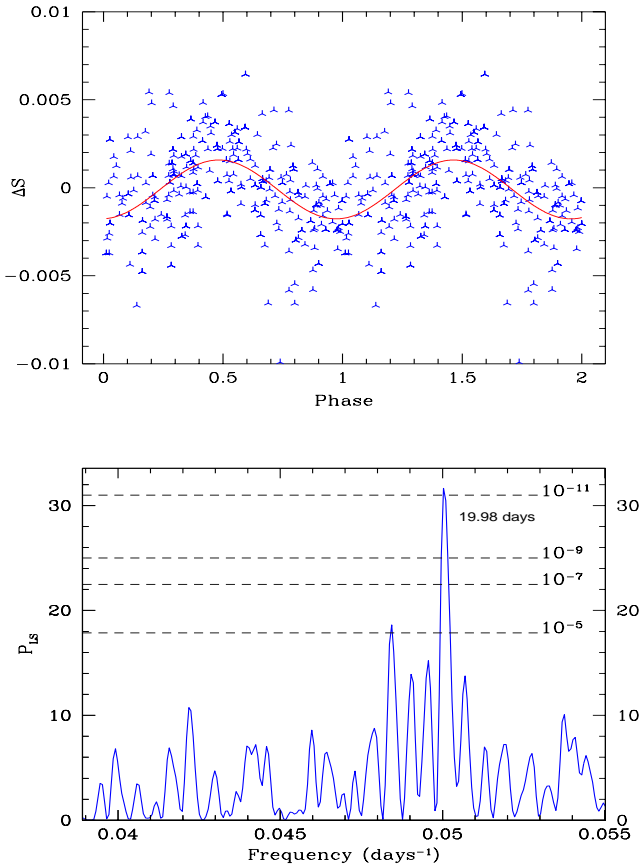


Fig. 7. Top panel: Mount Wilson index residuals phased with a period of ~ 19.98 days. Lower panel: Lomb–Scargle periodogram from filtered (residuals) Ca II H&K measurements. The highest peak suggests a rotation period 19.98 days.

4. Discussion

We studied the long-term activity of the solar-analog star HD 45184 by using the Ca II H&K and Balmer lines as stellar activity proxies. We analysed the Ca II H&K line-core fluxes in 291 HARPS spectra taken between 2003 and 2014. In addition, we detected spectral variability in the first 3 lines of the Balmer series and in some strong lines of ionized metals, particularly Fe II lines at 4924 Å, 5018 Å, and 5169 Å. We detected a long-term activity cycle of 5.14-yr from the Ca II H&K lines, which is clearly replicated by line profile variations in Balmer and strong Fe II lines (see e.g. Fig. 4). Equivalent width variations of Balmer (except for H α) and Fe II lines present a positive correlation with the emission in the Ca II H&K lines: the more intense the emission of the Ca II H&K lines, the stronger the H I and Fe II lines. In the case of H α , the equivalent width does not suffer significant changes, although the line profile shape varies in phase with the activity cycle.

It is believed that the surface of older and less active stars, including our Sun, are dominated by bright regions called faculae, whereas young and active stars are spot dominated (Radick et al. 1998; Berdyugina et al. 2002). Moore et al. (1966) showed a number of Fe lines sensitive to the presence of Sun spots. Based on this scenario and considering the similarities between the Sun and HD 45184, an Fe II variation following the Ca H&K activity cycle could be possibly attributed to the lower age of HD 45184.

This could be verified using future observations of other young solar-analog stars.

Solar spectral variation of several Fraunhofer lines along the 11-yr activity cycle were first revealed by Livingston & Holweger (1982). Next, taking into account that these lines are formed at different depths in the atmosphere of the Sun, Livingston et al. (2007) used some photospheric and chromospheric lines to study the long-term variations of the temperature. Monitoring high photospheric lines from 1980 to 2006, they found that Mn 5394 Å is the only photospheric line which shows a clear modulation with the chromospheric 11-yr Ca II K cycle of the Sun. Surprisingly, Fe lines did not show the expected modulation with Ca II H&K lines, and then they suggest that these lines are probably following the 22-yr Hale cycle. Interestingly, in HD 45184 we found that Fe II lines show a clear modulation with the 5.14-yr Ca II H&K activity cycle. Following Moore et al. (1966), the variations of these high photospheric Fe II lines could point toward the possible presence of dark spots in the surface of HD 45184. At the same time, and similar to the solar case, the faculae are presumably present on the stellar surface, as suggested by the Ca II H&K emission lines (e.g. Hall 2008, and references therein).

Using the Ca II H&K lines we found for short-term modulations caused by stellar rotation and determined a rotation period of 19.98 days for HD 45184. This value is in agreement with the rotational period vs. chromospheric activity calibration of Wright et al. (2004). On the other hand, being HD 45184 more active than the Sun, the rotation period calculated by us is expected to be shorter than the rotation period of Sun, because of the widely believed close connection between rotation and activity (Noyes et al. 1984).

Despite solar-twin and solar-analog stars are ideal laboratories to carry out comparative studies of stellar cycles and the solar cycle, not many of them have been considered as targets of activity studies. An interesting aspect of HD 45184 is that, among stars with detected activity cycles, it is one of which have stellar parameters closest to the solar values. In Fig. 8 we show the position in the $T_{\text{eff}} - \log g$ diagram of stars with known activity cycles. We have included G-type stars studied by Choi et al. (2015) and the Mount Wilson project stars selected by Schröder et al. (2013) as having cyclic variations. Additionally, we added individual objects with activity periods reported by Metcalfe et al. (2010), DeWarf et al. (2010), and Egeland et al. (2015). We included in the Figure the parameters of HD 45184 determined by different literature works (Sousa et al. 2008; Bensby et al. 2014; Battistini & Bensby 2015; Maldonado et al. 2015; Nissen 2015; Spina et al. 2016), using blue filled circles with error bars. For comparison, theoretical isochrones of Mowlavi et al. (2012) for solar abundances are plotted. HD 45184 has almost the same surface gravity as the Sun within the uncertainties and it is slightly hotter. In particular, Bensby et al. (2014) estimate an age of 4.4 ± 2.2 Gyr, similar to the age of the Sun. However, the parameters reported by Sousa et al. (2008) suggest that HD 45184 is about 2 Gyr younger than the Sun, in agreement with Nissen (2015). Without going in further detail, we can say that HD 45184 is ~ 100 K hotter than the Sun, and is one of the closest solar-analog stars with a known activity cycle.

It would be interesting to study if the Fe II lines could be also useful, for instance, to detect a possible activity cycle in those planet-search radial-velocity surveys that do not include the classical Ca II H&K lines in their spectra. This is the case, for example, of the Anglo-Australian Planet Search survey (e.g. Butler et al. 1996, 2001; Tinney et al. 2011). We caution, how-

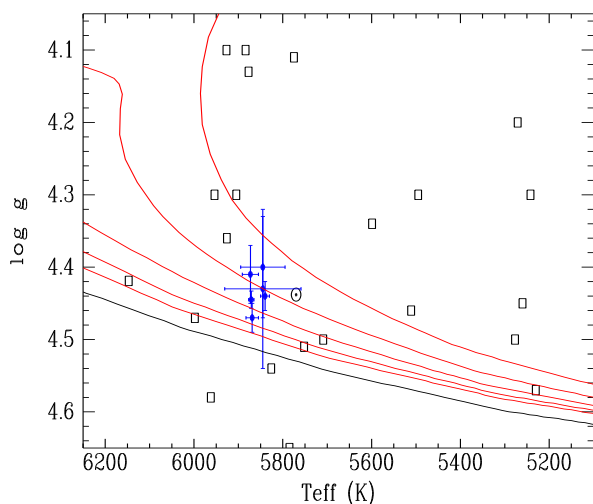


Fig. 8. Position of G-type stars with activity cycles in the $T_{\text{eff}} - \log g$ diagram (black empty squares). Blue filled circles with error bars correspond to the parameters of HD 45184 derived by different authors. Red lines are isochrones for solar abundances are shown for $\log \text{age} = 9.0, 9.2, 9.4, 9.6,$ and 9.8 ; black line is the ZAMS. The position of the Sun is also included in the figure.

ever, that more observations are needed to verify the usefulness of the Fe and possibly other metallic lines in solar-analog stars.

Acknowledgements. We thank the anonymous referee for constructive comments that improved the paper.

References

- Baliunas, S. & Jastrow, R. 1990, *Nature*, 348, 520
 Baliunas, S. L., & et al. 1995, *Astrophys. J.*, 438, 269
 Baliunas, S. L., Donahue, R. A., Soon, W., & Henry, G. W. 1998, in *ASP Conf. Ser. 154: Cool Stars, Stellar Systems, and the Sun*, ed. R. A. Donahue & J. A. Bookbinder, 153–+
 Battistini, C. & Bensby, T. 2015, *A&A*, 577, A9
 Bensby, T., Feltzing, S., & Oey, M. S. 2014, *A&A*, 562, A71
 Berdyugina, S. V., Pelt, J., & Tuominen, I. 2002, *A&A*, 394, 505
 Brown, K. I. T., Gray, D. F., & Baliunas, S. L. 2008, *ApJ*, 679, 1531
 Buccino, A. P. & Mauas, P. J. D. 2009, *A&A*, 495, 287
 Buccino, A. P., Petrucci, R., Jofré, E., & Mauas, P. J. D. 2014, *ApJ*, 781, L9
 Busà, I., Aznar Cuadrado, R., Terranegra, L., Andretta, V., & Gomez, M. T. 2007, *A&A*, 466, 1089
 Butler, R. P., Marcy, G. W., Williams, E., et al. 1996, *PASP*, 108, 500
 Butler, R. P., Tinney, C. G., Marcy, G. W., et al. 2001, *ApJ*, 555, 410
 Carolo, E., Desidera, S., Gratton, R., et al. 2014, *A&A*, 567, A48
 Choi, H., Lee, J., Oh, S., et al. 2015, *ApJ*, 802, 67
 Cincunegui, C., Díaz, R., & Mauas, P. 2007, *A&A*, 469, 309
 DeWarf, L. E., Datin, K. M., & Guinan, E. F. 2010, *ApJ*, 722, 343
 Duncan, D. K., Vaughan, A. H., Wilson, O. C., et al. 1991, *ApJS*, 76, 383
 Egeland, R., Metcalfe, T. S., Hall, J. C., & Henry, G. W. 2015, *ApJ*, 812, 12
 Gomes da Silva, J., Santos, N. C., Boisse, I., Dumusque, X., & Lovis, C. 2014, *A&A*, 566, A66
 Gomes da Silva, J., Santos, N. C., Bonfils, X., et al. 2011, *A&A*, 534, A30
 Gray, D. F. & Baliunas, S. L. 1995, *ApJ*, 441, 436
 Gray, R. O., Corbally, C. J., Garrison, R. F., et al. 2006, *AJ*, 132, 161
 Hall, J. C. 2008, *Living Reviews in Solar Physics*, 5
 Hall, J. C., Henry, G. W., & Lockwood, G. W. 2009, *AJ*, 138, 312
 Hall, J. C. & Lockwood, G. W. 1998, *ApJ*, 493, 494
 Hall, J. C., Lockwood, G. W., & Skiff, B. A. 2007, *AJ*, 133, 862
 Henry, T. J., Soderblom, D. R., Donahue, R. A., & Baliunas, S. L. 1996, *AJ*, 111, 439
 Horne, J. H. & Baliunas, S. L. 1986, *ApJ*, 302, 757
 Lawler, S. M., Beichman, C. A., Bryden, G., et al. 2009, *ApJ*, 705, 89
 Livingston, W. & Holweber, H. 1982, *ApJ*, 252, 375
 Livingston, W., Wallace, L., White, O. R., & Giampapa, M. S. 2007, *ApJ*, 657, 1137

- Lovis, C., Dumusque, X., Santos, N. C., et al. 2011, *arXiv: [arXiv:1107.5325]*
 Maldonado, J., Eiroa, C., Villaver, E., Montesinos, B., & Mora, A. 2015, *A&A*, 579, A20
 Martínez-Arnaiz, R., López-Santiago, J., Crespo-Chacón, I., & Montes, D. 2011, *MNRAS*, 414, 2629
 Martínez-Arnaiz, R., Maldonado, J., Montes, D., Eiroa, C., & Montesinos, B. 2010, *A&A*, 520, A79
 Mayor, M., Marmier, M., Lovis, C., et al. 2011, *ArXiv e-prints [ArXiv Astrophysics e-prints:1109.2497]*
 Metcalfe, T., Basu, S., Henry, T. J., et al. 2010, *ApJ*, 723, L213
 Metcalfe, T., Buccino, A., Brown, B., et al. 2013, *ApJ*, 763, L26
 Meunier, N. & Delfosse, X. 2009, *A&A*, 501, 1103
 Moore, C. E., Minnaert, M. G. J., & Houtgast, J. 1966, *The solar spectrum 2935 Å to 8770 Å*
 Mowlavi, N., Eggenberger, P., Meynet, G., et al. 2012, *A&A*, 541, A41
 Nissen, P. E. 2015, *A&A*, 579, A52
 Noyes, R. W., Hartmann, L. W., Baliunas, S. L., Duncan, D. K., & Vaughan, A. H. 1984, *ApJ*, 279, 763
 Pietarila, A. & Livingston, W. 2011, *ApJ*, 736, 114
 Radick, R. R., Lockwood, G. W., Skiff, B. A., & Baliunas, S. L. 1998, *ApJS*, 118, 239
 Reiners, A., Joshi, N., & Goldman, B. 2012, *AJ*, 143, 93
 Robertson, P., Endl, M., Cochran, W. D., & Dodson-Robinson, S. E. 2013a, *ApJ*, 764, 3
 Robertson, P., Endl, M., Cochran, W. D., MacQueen, P. J., & Boss, A. P. 2013b, *ApJ*, 774, 147
 Schröder, K.-P., Mittag, M., Hempelmann, A., González-Pérez, J. N., & Schmitt, J. H. M. M. 2013, *A&A*, 554, A50
 Sokolov, N. A. 2000, *A&A*, 353, 707
 Sousa, S. G., Santos, N. C., Mayor, M., et al. 2008, *A&A*, 487, 373
 Spina, L., Meléndez, J., & Ramírez, I. 2016, *A&A*, 585, A152
 Stellingwerf, R. F. 1978, *ApJ*, 224, 953
 Stelzer, B., Frasca, A., Alcalá, J. M., et al. 2013, *A&A*, 558, A141
 Tinney, C. G., Butler, R. P., Jones, H. R. A., et al. 2011, *ApJ*, 727, 103
 van Leeuwen, F. 2007, *A&A*, 474, 653
 Vaughan, A. H., Preston, G. W., & Wilson, O. C. 1978, *MNRAS*, 90, 267
 Wilson, O. C. 1978, *ApJ*, 226, 379
 Wright, J. T., Marcy, G. W., Butler, R. P., & Vogt, S. S. 2004, *ApJS*, 152, 261